European Journal of Pharmaceutics and Biopharmaceutics 71 (2009) 257–263

Contents lists available at ScienceDirect

European Journal of Pharmaceutics and Biopharmaceutics

journal homepage: www.elsevier.com/locate/ejpb

Research paper

Chitosan/cyclodextrin nanoparticles can efficiently transfect the airway epithelium in vitro

Desirée Teijeiro-Osorio, Carmen Remuñán-López, María José Alonso *

Department of Pharmacy and Pharmaceutical Technology, University of Santiago de Compostela, Santiago de Compostela, Spain

ARTICLE INFO

Article history:
Received 29 March 2008
Accepted in revised form 22 September 2008
Available online 14 October 2008

Keywords:
Calu-3 cells
Chitosan
Cyclodextrin
Nanoparticles
Nanocarriers
Gene/DNA delivery

ABSTRACT

The main goal of the present study was to investigate the potential of a new generation of hybrid polysaccharide nanocarriers, composed of chitosan (CS) and anionic cyclodextrins (CDs), for gene delivery to the airway epithelium. More specifically, these nanocarriers were investigated with regard to their ability to enter epithelial cells and promote gene expression in the Calu-3 cell culture model.

In the search for the most suitable nanocarrier composition for gene delivery, the effect of CS molecular weight (Mw) on the nanocarriers characteristics and their ability to transfect cells was investigated. Thus, hybrid CS/CD nanoparticles were prepared with two different CS Mw, medium (110 kDa) and low (10 kDa), and loaded with pSEAP (plasmid DNA model that encodes the expression of secreted alkaline phosphatase). The resulting nanoparticles presented an adequate size range (100–200 nm, depending on CS Mw), a positive surface charge (+22 to +35 mV) and very high DNA association efficiency values (>90%). Cellular uptake studies showed that the nanoparticles were effectively internalized by the cells, providing a good indication of their potential as gene carriers. The transfection efficiency of the different formulations, measured by the concentration of secreted gene product (SEAP), indicated that all the nanoparticles were able to elicit a significantly higher response than the naked DNA (control), the transfection efficiency being more important for low MwCS nanoparticles than for those composed of medium MwCS. Overall, this report is the first evidence of the potential of a new generation of safe polysaccharide nanocarriers for gene delivery to the airway epithelium.

1. Introduction

Over the last few years, there has been an increasing interest in the delivery of genes to the airway epithelium, either for therapeutic (e.g. cystic fibrosis, α1-antitripsin deficiency) or for vaccination purposes [1–3]. In spite of the advances made in facilitating the delivery of drugs to the nasal/bronchial epithelium, there are still important barriers to overcome before achieving a successful gene transfer in these respiratory regions. Probably, the most critical barriers are represented by the mucus-gel layer involved in the mucociliary clearance mechanisms and the low rate of endocytosis taking place on the apical side of airway epithelial cells [4,5].

Currently, the transport of exogenous DNA to cells can be accomplished by using viral and non-viral vectors. Although both gene delivery systems are under investigation, virus-based gene therapy is limited by concerns about endogenous virus recombinations, oncogenic effects and immunological reactions [6]. Alternatively, the non-viral gene delivery agents offer several advantages, including easiness in production and low cost, safety, and lack of immunogenicity. However, their use has been limited by their relatively low transfection efficiency in vivo [7,8].

Most commonly, the non-viral systems consist of ionic complexes formed by the condensation of DNA through electrostatic interactions with cationic polymers (polyplexes) or lipids (lipoplexes). Among cationic polymers, chitosan (CS), which is a natural linear polysaccharide obtained by the partial deacetylation of chitin, exhibits several favorable biological properties, such as biodegradability, low toxicity, biocompatibility and mucoadhesiveness [9]. Although CS polyplexes are promising for mucosal gene delivery, they still suffer from several limitations, such as undefined physical shapes, dissociation of the complexes in the presence of anions and a limited capacity to co-associate other functional molecules that could help to achieve efficient gene transfer and expression. As an alternative, our research group and others have recently reported the preparation of CS nanoparticles formed by ionic gelation with tripolyphosphate (TPP) as delivery systems for DNA [10,11] and siRNA [12]. These nanoparticles consisting of CS were able to associate high amounts of genetic material and provided high gene expression levels both in vitro and in vivo.

* Corresponding author. Department of Pharmacy and Pharmaceutical Technology, University of Santiago de Compostela, Faculty of Pharmacy, Campus Sur, 15782-Santiago de Compostela, Spain. Tel.: +34 981 563100x14885; fax: +34 981 547148.
E-mail address: mjosefa.alonso@usc.es (M.J. Alonso).

0939-6411/$ - see front matter © 2008 Elsevier B.V. All rights reserved.
doi:10.1016/j.ejpb.2008.09.020

Recently, we reported a new generation of polysaccharide nanocarriers consisting of the polysaccharide CS and cyclic oligosaccharides named cyclodextrins (CDs) [13–15]. The rational behind the design of these new nanocarriers was to combine the promising behaviour of CS nanoparticles with the excellent biopharmaceutical properties of CD. Indeed, CDs are very well known in the pharmaceutical field because of their ability to protect drugs from physical, chemical and enzymatic degradation, and to enhance membrane permeability [16,17]. Currently, there are several kinds of neutral, amphiphilic and cationic CD, which can be used for the design of novel gene delivery systems. For example, CDs have also been conjugated with polycationic polymers, such as polyamidine and polyethylenimine, and dendrimers, to form polyplexes, which were found to elicit an increased transfection efficiency and stability against enzymatic degradation with low in vitro and in vivo toxicity [17–20].

Bearing all this information in mind, we hypothesized that the incorporation of CDs to the already effective CS-based gene delivery nanocarriers could positively contribute to: (a) promote cellular uptake, and (b) decrease the cytotoxicity of the systems.

The aim of the present work was to investigate the potential of CS/CD nanoparticles as gene delivery systems to the airway epithelium. For this purpose, different nanoparticulate compositions of CS and CD (different CS Mw and different anionic CD derivatives) were prepared and characterized. The nanoparticle cytotoxicity and ability to enter and transfect cells in vitro was evaluated in the human mucus-producing cell line Calu-3, a model for the nasal and bronchotracheal airway epithelium, recently proposed as an adequate model for gene delivery [21].

2. Materials and methods

2.1. Materials

Ultrapure chitosan (CS) hydrochloride salt (Protasan UP CL 113, having a molecular weight of around 110 kDa and deacetylation degree = 86%) was purchased from FMC Biopolymers (Norway). Cyclodextrin (CD) anionic derivatives, sulfobutylether-β-CD (SBE-β-CD, substitution degree ≈ 7) and carboximethyl-β-CD (CM-β-CD, substitution degree = 3.0–3.5) were purchased from Cydex Inc. (USA) and Fluka Biochem (France), respectively. Plasmid DNA (pDNA) encoding secreted alkaline phosphatase (pSEAP) based on the gWiz™ high-expression vector system was purchased from Aldevron (USA). Eagle's Minimum Essential Medium (MEM) was purchased from ATCC (BMG Laboratory, Spain). Foetal Bovine Serum (FBS), penicillin/streptomycin (100 μg/mL), MTT ((3-4,5-dimethylthiazol-2-yl)-2,5-diphenyltetrazolium bromide), fluorescein sodium salt, and pentasodium tripolyphosphate (TPP) were all obtained from Sigma–Aldrich (Spain). Phosphate-buffered saline (PBS), Hanks' balanced salt solution (HBSS) 1× and 10× were purchased from Gibco™ (UK). One KBp DNA ladder was obtained from Life Technologies (Spain). Triton® X-100 and DMSO was acquired from Fluka Biochem. (Spain). 12-well tissue culture plates with cell culture inserts (0.9 cm^2, 0.4 μm pore size) and flat-bottomed 96-well plates were obtained from Falcon™ (Becton–Dickinson Labware, USA). Ultrapure water (MilliQ Plus, Millipore Iberica, Spain) was used throughout. All other solvents and chemicals were of the highest grade commercially available.

2.2. Preparation of fluorescein-labelled chitosan (Fl-CS)

CS was labelled with fluorescein, following a slightly modified method described by De Campos et al. [22]. The covalent attachment of fluorescein to CS was achieved by the formation of amide bonds between primary amino groups of the polymer and the carboxylic acid groups of fluorescein. Briefly, 250 mg of CS was dissolved in 25 mL of water, and an amount of 10 mg of fluorescein was dissolved in 1 mL of ethanol. Thereafter, both solutions were mixed together and to catalyse the formation of amide bonds, EDAC (1-ethyl-3-(3-dimethylaminopropyl) carbodiimide hydrochloride) was added in a final concentration of 0.05 M. The reaction mixture was incubated under permanent magnetic stirring for 12 h in the dark at room temperature. The resulting conjugate (Fl-CS) was isolated by exhaustive dialysis (cellulose dialysis tubing, pore size 12,400 Da; Sigma–Aldrich, Spain) against demineralised water and then freeze-dried.

2.3. Depolymerization of chitosan

Low molecular weight CS (LMwCS) was obtained from Protasan UP CL 113 by sodium nitrite degradation as previously described [23]. Briefly, 200 μL of 0.1 M $NaNO_2$ was added to 4 mL of the CS solution (10 mg/mL) at room temperature under magnetic stirring. The reaction mixture was left overnight to assure the completion of the degradation, and fragments with an approximate Mw of 10 kDa were recovered by freeze-drying. The molecular size of the LMwCS was verified by size exclusion chromatography (SEC).

2.4. Nanoparticle preparation

Nanoparticles were spontaneously obtained by ionotropic gelification [24]. Two aqueous phases containing: (1) the CS solution (CS, Fl-CS or LMwCS), and (2) the CD solution (SBE-β-CD or CM-β-CD) with the cross-linker TPP, were mixed under magnetic stirring and maintained under agitation for 10 min to allow the complete formation of the system. The CS, Fl-CS or LMwCS solutions were prepared at a concentration of 2 mg/mL, and the volume employed was fixed at 3 mL. On the other hand, in order to modulate the mass ratio of the components that constituted the nanoparticles (CS/CD/TPP), the corresponding volumes of the CD aqueous solution (SBE-β-CD or CM-β-CD, 6–12 mg/mL) and TPP solution (1.5 mg/mL) were mixed at a final volume of 1 mL.

For nanoparticles encapsulating a pDNA model, the required amount of the plasmid encoding secreted alkalin phosphatase (gWiz™pSEAP) was incorporated directly in the CD/TPP phase. The theoretical loadings were fixed at 5% (w/w).

As a control, nanoparticles composed solely by CS and TPP were prepared by the same method and loaded by including the corresponding amount of pDNA model in the TPP solution.

2.5. Nanoparticle characterization

The mean particle size and the size distribution of the nanoparticles were determined by Photon Correlation Spectroscopy (PCS). The zeta potential values of the nanoparticles were obtained by Laser Doppler Anemometry (LDA), measuring the mean electrophoretic mobility. Samples of the nanoparticle suspensions were diluted at the appropriate concentration with filtered water for PCS and with 1mM KCl for LDA. PCS and LDA analyses were performed with a Zetasizer® 3000 HS (Malvern Instruments, UK).

Eventually, nanoparticles were concentrated by centrifugation (Beckman Avanti TM 30, Beckman, Spain) on a glycerol bed. In order to resuspend the nanoparticles at the required concentration, the amount of nanoparticles in the sediment was calculated by weight upon their freeze-drying.

The association of pDNA to the nanoparticles was studied by a conventional agarose gel electrophoresis assay. Samples of the nanoparticles were placed in 1% agarose gel containing ethidium bromide, and ran for 90 min at 60 V in TAE buffer (Sub-Cell GT 96/192, Bio-Rad Laboratories Ltd., England).

2.6. Cell culture

Calu-3 cells were purchased from American Type Culture Collection ATCC (Rockville, USA) and grown in MEM (supplemented with 10% FBS and 100 μg/mL penicillin/streptomycin) at 37 °C in a 5% CO_2 humidified atmosphere. Cells were detached from culturing flasks by trypsin-EDTA and subcultivated for studies with proliferating cells or with a well-differentiated epithelium. For cytotoxicity studies with proliferating cells, the cells were seeded in flat-bottomed 96-well culture plates in a density of 6×10^4 cells/well and cultured for 72 h. To obtain a differentiated epithelium, cells were cultured on inserts with a density of 2×10^5 cells/cm^2 (0.9 cm^2/insert). Post seeding onto the filter, the Calu-3 cells attached to the filter overnight and the medium was then removed from the apical compartment to allow the cells to form a monolayer at an air-liquid interface. The differentiation stage during cultivation was followed by measuring the transepithelial electric resistance (TEER) (Millicell®-ERS, Millipore Corp., USA). After 15–18 days the differentiated cells, with mean TEER values around 1100–1200 Ω cm^2, were used in cellular uptake studies and transfection experiments with pSEAP. Pass numbers 28–40 were used for the following experiments.

2.7. Cytotoxicity studies

The effect of different nanoparticle compositions and concentrations on cellular viability of proliferating Calu-3 cells was determined by MTT colorimetric assay, which was conveniently optimized. MTT is a yellow tetrazolium salt that is reduced only in living, metabolically active cell mitochondria. Cells grown in 96-well culture plates were washed twice with 100 μL of HBSS, and the test nanoparticle suspensions (100 μL, in HBSS, pH 6.4) were added in concentrations ranging from 0.0125 to 2.5 mg/mL to the wells. At the end of the incubation time (2 h, 37° C) and according to extensive pretests, samples were discarded and replaced by 25 μL of MTT solution (5 mg/mL) and 100 μL of HBSS, pH 7.4. The plates were further incubated for 4 h at 37° C (protected from light), and the MTT solution was removed. The blue crystals formed in each well were dissolved with 100 μL of DMSO. Positive (Triton® X solution, 2% w/v) and negative (HBSS) control wells were treated similarly as above. Absorbance values were measured at 570 nm using a microplate reader. Cell viability, as a percent of the negative control, was calculated from the absorbance values. The IC_{50} was defined as the sample concentration inhibiting 50% cell viability. Analysis of four replicates was conducted in two different passages of cells ($n = 8$).

2.8. Uptake studies

Nanoparticles were prepared with a fluorescein-labelled CS (Fl-CS) according to the procedure described before, suspended in trehalose (5% w/v) and then added to the Calu-3 differentiated cells. After 1h incubation at 37° C, samples were removed and cells were rinsed three times with HBSS. Samples were fixed with 4% paraformaldehyde, permeabilised with 0.1% Triton® X and the cell nuclei were stained with propidium iodide according to manufacturers' instructions, including the ribonuclease A pre-treatment. Thereafter, the filters were cut and examined under Confocal Laser Scanning Microscopy (CLSM) (Leica TCS SP2, Leica GmbH, Germany), which allowed the simultaneous visualization of the two different fluorescent markers. Excitation wavelengths were 488 nm for fluorescein and 633 nm for propidium iodide.

2.9. Transfection studies

Transfection studies were performed with nanoparticles loaded with 5% (w/w) gWiz™pSEAP and naked pDNA (control) (2 μg/insert), placed on the apical compartment and incubated for 4 h. The yield of gene expression was non-invasively evaluated by monitoring concentrations of secreted alkaline phosphatase (SEAP) in the basolateral compartment at different time points. The first samples were taken immediately after the incubation of cells with the formulations, transferred to 1.5 mL eppendorf tubes and stored at −20° C. Remaining medium from the basolateral compartment and solutions from the apical compartment were removed. Both sides were washed with PBS, and fresh culture medium was applied on the basolateral side. Thereafter, samples were taken in the same manner for 6 days ($t = 1$, 2, 4 and 6 days). Finally, the samples were analyzed for SEAP quantification with a fluorescence assay using the Great EscAPe™ SEAP Reporter System Kit protocol (BD Biosciences Clontech, USA) and Fluorimeter (LS 50B Luminescence Spectrometer, Perkin-Elmer, USA).

2.10. Statistical analysis

Statistical differences were investigated using one-way ANOVA, followed by the Student–Newman–Keuls method for multiple comparisons. All analyses were run using the SigmaStat statistical program (version 3.1), and differences between the groups were judged significant at $P < 0.05$.

3. Results and discussion

As indicated in the introduction, the overall goal of this work was to assess the potential of a new nanocarrier based on biodegradable and non-toxic poly and oligosaccharides as a vehicle for the delivery of genes to the airway epithelia. To reach this goal several stages need to be taken into consideration:

(i) the ability to associate genes to the proposed nanocarrier without altering the inherent properties of the gene and also of the carrier;
(ii) the interaction of the nanocarrier with the selected target cells (Calu-3 cells);
(iii) the capacity of the gene-loaded nanocarrier to achieve cell transfection.

These three stages will be analyzed in detail in this specific section.

3.1. Definition of nanocarriers formation conditions and their ability to associate pDNA

CS and CS/CD nanoparticles were prepared by ionic gelation in the presence of TPP, as described in the methodology section. The mechanism of formation of the nanosystems combines the electrostatic interaction between CS and CDs, which are oppositely charged, with the ability of CS to undergo a liquid–gel transition due to its ionic interaction with TPP. As we postulated that the incorporation of CD would benefit the system properties, preliminar experiments were aimed at finding the maximum CS/CD mass ratio in which nanoparticles formed can be conveniently isolated, resuspended and characterized. This maximum ratio was found to be 4/3 (w/w) for CS/SBE-β-CD and 4/4 for CS/CM-β-CD. This great and different incorporation capacity of CD could be determined by their degree of substitution (DS), which is higher in SBE-β-CD (average DS = 6.4) than in CM-β-CD (DS = 3.0–3.5).

As shown in Table 1, all particles were in the nanometric range (234–358 nm) and exhibited a positive zeta potential (+35 to +17 mV); however, these properties were dependent on the composition. The smallest size was observed for CS/SBE-β-CD nanoparticles. This could be due to the fact that SBE-β-CD can be more substituted than CM-β-CD, and consequently led to the formation of more compacted and, thus, smaller nanostructures. As expected, a decrease in the surface charge was found in nanoparticles containing CD compared to those made solely by CS. The lowest value was observed for nanoparticles containing CM-β-CD, thus indicating the presence of an important amount of CD on the surface of the nanoparticles.

Once we defined the appropriate conditions for the formation of the nanoparticles, we studied the possibility to efficiently associate pSEAP, a pDNA model that encodes the expression of secreted alkaline phosphatase. With this idea in mind, we explored the influence of CS Mw on the characteristics of the nanoparticles and, afterwards, on their ability to transfect cells. More specifically, we chose CS, ≈110 kDa (Protasan UP CL 113) and low molecular weight CS (LMwCS, ≈10 kDa), obtained by partial depolymerization of the previous one. On the other hand, we fixed the theoretical pDNA loading at 5% (w/w, based on the weight of all nanoparticle components: CS or LMwCS, CD and TPP) and we used nanoparticles made of solely CS as a control, given their reported efficacy for gene delivery [10,11].

As shown in Table 2, all the formulations were in the desired nanometric range, presenting low polydispersity and positive zeta potential values. It can also be noted that nanoparticles made of LMwCS presented a lower positive zeta potential and a smaller size than those made of regular CS. This fact agrees with the previous results on CS nanoparticles prepared by ionic gelation [23,12,10]. The effect of CS Mw on the nanoparticle size could be related to the greater ability of lower MwCS molecules to organize forming smaller structures. Moreover, the smaller size and higher solubility of LMwCS could lead to a more efficient interaction with the pDNA, thus resulting in the formation of smaller particles [12,10].

The ability of the polysaccharide nanoparticles to entrap pDNA was studied using the agarose electrophoresis technique. From the photograph of the obtained agarose gel, depicted in Fig. 1, it could be stated that most of the DNA was associated to the nanoparticles, since no migration of free DNA was observed. This fact is in agreement with the previous results obtained for other CS-based nanometric systems, and it can be easily explained by the high affinity

Table 1
Physicochemical characteristics of nanoparticles composed solely by CS or CS and two different CD derivatives (SBE-β-CD, CM-β-CD) (means ± SD, $n = 3$).

CD type	CS/CD/TPP mass ratio	Size (nm)	PI[a]	Zeta potential (mV)
SBE-β-CD	4/3/0.25	264 ± 18	0.2–0.3	+27 ± 0.6
CM-β-CD	4/4/0.25	358 ± 13	0.4–0.5	+17 ± 2.2
–	4/0/1	335 ± 18	0.3–0.4	+35 ± 0.9

[a] PI, polydispersity index.

Table 2
Physicochemical characterization of 5% gWiz™pSEAP-loaded nanoparticles consisting of two different CS Mw (110 kDa and 10 kDa) and two different CD derivatives (SBE-β-CD, CM-β-CD) (means ± SD, $n = 3$).

CD type	CS/CD/TPP mass ratio	Size (nm)	PI[a]	Zeta potential (mV)
SBE-β-CD	4/3/0.25	180 ± 2	0.1–0.2	+35 ± 6
CM-β-CD	4/4/0.25	234 ± 15	0.1–0.2	+25 ± 5
–	4/0/1	192 ± 25	0.2–0.3	+34 ± 5
SBE-β-CD	4/1.5/0.25	143 ± 2	0.0–0.1	+24 ± 4
CM-β-CD	4/3/0.25	140 ± 8	0.0–0.1	+22 ± 6

[a] PI, polydispersity index.

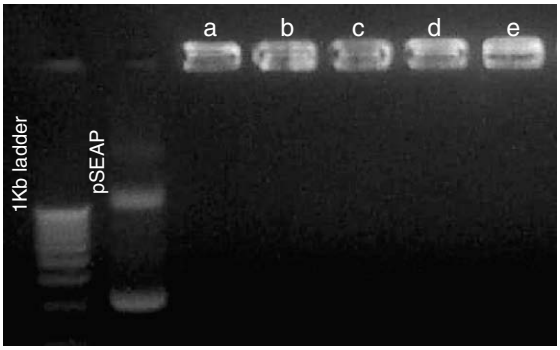

Fig. 1. Agarose gel electrophoresis of the different nanoparticles encapsulating plasmid DNA: (a) CS/SBE-β-CD/TPP; (b) CS/CM- β -CD/TPP; (c) CS/TPP; (d) LMwCS/SBE-β-CD/TPP; (e) LMwCS/CM- β -CD/TPP. 1 kb DNA ladder and untreated gWiz™pSEAP were used as control.

of CS for the DNA [11,25]. Indeed, it is known that the strong electrostatic interaction exists between the phosphate groups of DNA and the amino groups of CS, as well as hydrophobic and hydrogen bonds [26].

Consequently, overall these data show the possibility of modulating the composition of these novel nanocarriers going from a low to a very high CD content; all with adequate physicochemical properties in terms of size, polydispersity and zeta potential, and a very high pDNA association capacity.

3.2. Study of the toxicity of the nanocarrier and its interaction with the selected target cells (Calu-3 cells)

A critical step towards the design of a new pDNA carrier is the information on its ability to enter the target cells. However, since this ability is often connected with cytotoxicity, it is important first to evaluate the toxicity of these new nanocarriers in the Calu-3 cell line model (proliferating cells). We chose cells in the proliferating stage due to their greater sensitivity against toxic materials than the well differentiated cells [27].

The percentage of cell viability as a function of the administered nanoparticle dose (μg/cm^2) is depicted in Fig. 2. It can be noted that CS/CD nanoparticles exhibit a significantly lower cytotoxicity than those composed of solely CS. More specifically, the estimated IC_{50} values, which are the nanoparticle doses causing a reduction of 50% cell viability, were 3-fold higher for CD-containing nanoparticles than for the CS control nanoparticles. This very good viability profile exhibited by this new generation of polysaccharide nanoparticles would be easily explained by the good safety record of CD [17]. Moreover, when comparing both types of CD-containing

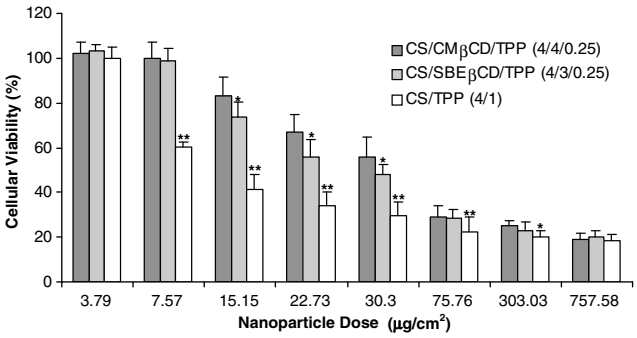

Fig. 2. Sensitivity of Calu-3 proliferating cells toward various doses of different nanoparticle formulations (CS/SBE-β-CD/TPP, CS/CM-β-CD/TPP, CS/TPP) determined by the MTT assay (means ± SD, $n = 8$). *Denotes significant differences ($P < 0.05$).

nanoparticles, we observed a significantly lower toxicity for those containing CM-β-CD than those containing SBE-β-CD.

In the second stage, once the cytotoxicity of the nanocarriers was known, we studied the interaction of nanoparticles with the Calu-3 cells. For this specific type of study differentiated rather than proliferating cells were selected. The Calu-3 differentiated cells are considered as an appropriate model for the nasal and bronchotracheal airway epithelia because of its features in the normal human tissues, such as tight junctions, high TEER values and mucous excretions [21]. Additionally, as previously mentioned in the methodology section, Calu-3 differentiated cells were cultured at an air–liquid interface (removal of apical culture medium 1 day after seeding), in order to reproduce the physiological situation better [28,29].

The study of the interaction of the nanocarriers with the cells was performed by confocal fluorescence microscopy. Therefore, for the purpose of this study we also developed fluorescent nanoparticles from a fluorescent CS derivative (Fl-CS). The results showed that the labelling procedure did not alter the physicochemical properties of the nanoparticles.

The Calu-3 monolayer was then exposed to the fluorescent nanoparticles, and the cell nuclei were stained with propidium iodide in order to facilitate the localization of the particles in the cells. As noted by the localization of the green signal corresponding to the nanoparticles, the CLSM images depicted in Fig. 3a (x–y sections) indicate that irrespective of their composition, the nanoparticles were effectively internalized by the cells. The localization of the nanoparticles can be better visualized in the x–z cross-sections of the cells, in which the green fluorescence derived from the nanoparticles can be localized around the cell nuclei (red emission) (example shown in Fig. 3b). These results are in accordance with the previous studies reported by our group for CS nanoparticles [10] and CS/hyaluronic acid nanoparticles [25], and provide a good indication of their potential as gene carriers. The mechanism of this transcellular penetration is thought to occur predominantly by adsorptive endocytosis indicated by nonspecific interactions between nanoparticles and cell membranes [30].

3.3. Study of the capacity of the gene-loaded nanocarrier to achieve cell transfection

Following the observation of the capacity of the nanocarriers to enter the cells, and with the final goal of exploring their potential in gene therapy, we studied their ability to transfect the cell monolayer. It should be pointed out that the in vitro transfection studies are commonly carried out in proliferating and fast-growing cells, which are relatively easy to transfect. In contrast, the well-differentiated cells, which represent a more adequate model of the in vivo situation, are difficult to transfect since they are not prepared to easily accept a foreign pDNA [21]. Therefore, we selected these Calu-3 differentiated cells as a useful tool for predicting their future real possibilities in gene therapy.

For this study, we used a non-invasive method previously reported for epidermal (REK cells) and corneal (HCE cells) cell culture models [31,32]. More specifically, the nanoparticles containing pSEAP were added to the monolayer and the amount of alkaline phosphatase produced by the cells and, then, secreted to the culture medium was determined for up to 6 days. The nanoparticle dose selected for this study was of 45 μg/cm^2, which resulted in a cellular viability within 90–100% in differentiated Calu-3 cells (data not shown).

As shown in Figs. 4 and 5, transfection with naked pDNA produced very low gene expression, whereas all the nanoparticle formulations were able to elicit a significantly higher response. This fact can also be clearly noted in Table 3, which depicts the pharmacokinetic parameters of SEAP secretion by the monolayer. The

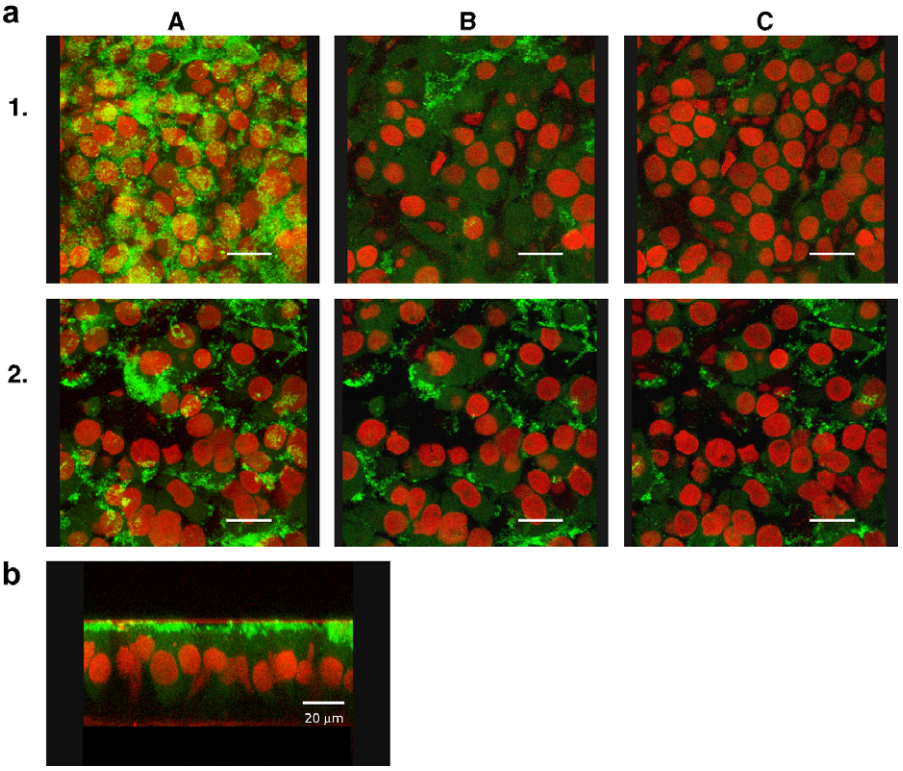

Fig. 3. (a) Confocal laser scanning microphotographs of Calu-3 cells incubated with (1) CS/CM-β-CD/TPP and (2) CS/SBE-β-CD/TPP nanoparticles prepared with fluorescein-labelled chitosan (Fl-CS, green channel), x–y cross-sections: (A) epithelium surface, (B) 5 μm, and (C) 10 μm. Cell nuclei are stained with propidium iodide (red channel). Scale bar represents 20 μm. (b) Confocal laser scanning microphotographs of Calu-3 cells incubated with CS/CM-β-CD/TPP nanoparticles prepared with fluorescein-labelled chitosan (Fl-CS, green channel), x–z section. Cell nuclei are stained with propidium iodide (red channel).

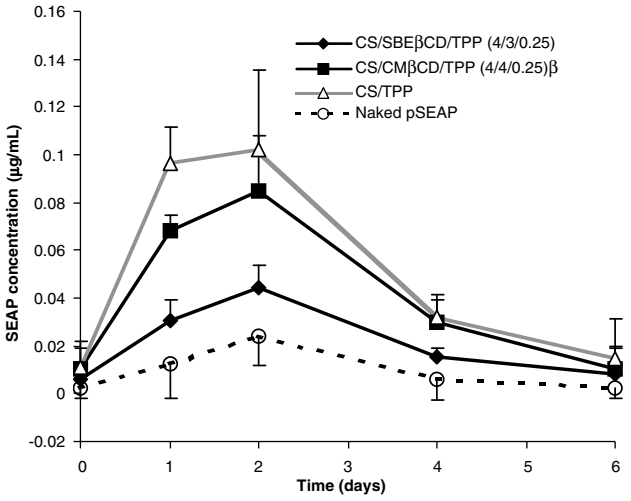

Fig. 4. Secreted alkaline phosphatase (SEAP) concentration in the Calu-3 cell culture model after transfection with naked pDNA and three different nanoparticle formulations (CS/SBE-β-CD/TPP; CS/CM-β-CD/TPP; and CS/TPP) encapsulating pDNA (means ± SD, $n = 5$).

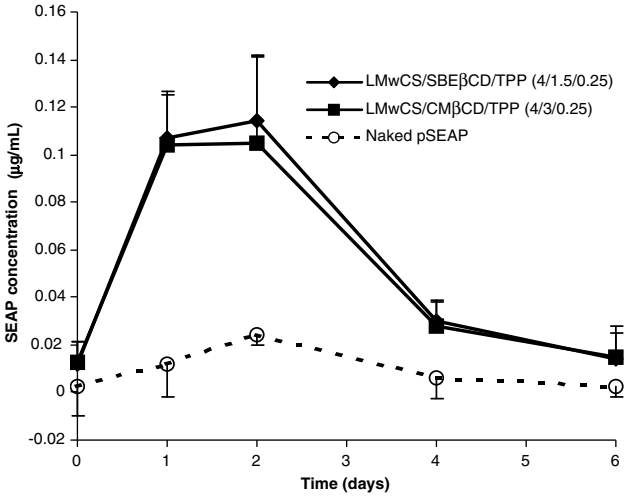

Fig. 5. Secreted alkaline phosphatase (SEAP) concentration in the Calu-3 cell culture model after transfection with naked pDNA and two different nanoparticle formulations (LMwCS/SBE-β-CD/TPP; LMwCS/CM-β-CD/TPP) encapsulating pDNA (means ± SD, $n = 5$).

Table 3
Pharmacokinetic parameters of the SEAP expression by the Calu-3 cell culture model after transfection with naked DNA (gWiz™pSEAP) and several nanoparticle formulations (means ± SD, $n = 5$).

Formulation	C_{max} (μg/mL)	Cumulative SEAP secretion[a] (μg)	AUC (μg h/mL)
gWiz™pSEAP	0.024 ± 0.01	0.045 ± 0.01	2.33 ± 0.41
CS/SBE-β-CD/TPP	0.044 ± 0.01	0.101 ± 0.03	4.39 ± 1.76
CS/CM-β-CD/TPP	0.084 ± 0.02	0.202 ± 0.02	10.16 ± 0.93
CS/TPP	0.102 ± 0.03	0.255 ± 0.05	12.50 ± 2.33
LMwCS/SBE-β-CD/TPP	0.113 ± 0.03	0.276 ± 0.04	13.45 ± 1.61
LMwCS/CM-β-CD/TPP	0.105 ± 0.04	0.264 ± 0.04	12.72 ± 1.60

[a] After 6 days.

maximum transfection levels were observed at 2 days post-incubation in all cases. The comparison of the efficiency of the nanocarrier prototypes (Fig. 4) led us to the conclusion that the nanocarriers composed by CS and CM-β-CD are the most promising, since they elicit values which are close to those of positive control (CS nanoparticles). The lower efficacy of CS/SBE-β-CD nanoparticles could be related to the strong electrostatic interaction between CS and SBE-β-CD, which may prevent the intracellular DNA release. Interestingly, this reduced efficacy was not observed for the nanoparticles made of LMwCS (Fig. 5), in which both prototypes containing either SBE-β-CD or CM-β-CD elicited a similar and high expression level. Moreover, this response was significantly higher than the one obtained with the original CS (Mw 110 kDa) (Fig. 4 and Table 3). These results agree with those reported by other authors, who have also related the higher efficacy of nanoparticles and polyplexes composed of low MwCS with the easier intracellular release of the pDNA [33,10]. A similar finding was described by De la Fuente et al. for the nanoparticles composed of hyaluronic acid and different CS Mw [32].

To summarize, this final step of the work represents clear evidence of the ability of this new generation of polysaccharide nanocarriers to transfect complex and structured cell monolayers such as the Calu-3 monolayer.

4. Conclusions

In this work, we present a new generation of polysaccharide nanocarriers consisting of CS and CD as a non-viral gene delivery system. Besides their great pDNA association capacity, these nanoparticles exhibit a low cytotoxicity and the ability to enter the cells, deliver the associated DNA and elicit high levels of protein expression. Consequently, these nanocarriers represent a promising approach for gene therapy at the level of mucosal surfaces and, in particular the respiratory mucosa.

Acknowledgements

This work has been supported by the European Commission within the 6th Framework programme – NanoBiosaccharides – Contract nr. 013882. The first author acknowledges the pre-doctoral fellowship granted by this Program.

References

[1] S.M. Graham, J.L. Launspach, Utility of the nasal model in gene transfer studies in cystic fibrosis, Rhinology 35 (1997) 149–153.
[2] K.L. Brigham, K.B. Lane, B. Meyrick, A.A. Stecenko, S. Strack, D.R. Cannon, M. Caudill, A.E. Canonico, Transfection of nasal mucosa with a normal alpha$_1$-antitrypsin gene in alpha$_1$-antitrypsin-deficient subjects: comparison with protein therapy, Human Gene Ther. 11 (2000) 1023–1032.
[3] U. Griesenbach, R.L. Cassady, S. Ferrari, M. Fukumura, C. Müller, E. Schmitt, J. Zhu, P.K. Jeffery, Y. Nagai, D.M. Geddes, M. Hasegawa, E.W.F.W. Alton, The nasal epithelium as a factory for systemic protein delivery, Mol. Ther. 5 (2002) 98–103.
[4] R.J. Pickles, D. McCarty, H. Matsui, P.J. Hart, S.H. Randell, R.C. Boucher, Limited entry of adenovirus vectors into well-differentiated airway epithelium is responsible for inefficient gene transfer, J. Virol. 72 (1998) 6014–6023.
[5] J.L. Lemoine, R. Farley, L. Huang, Mechanism of efficient transfection of the nasal airway epithelium by hypotonic shock, Gene Ther. 12 (2005) 1275–1282.
[6] D. Lee, W. Zhang, S.A. Shirley, X. Kong, G.R. Hellermann, R.F. Lockey, S.S. Mohapatra, Thiolated chitosan/DNA nanocomplexes exhibit enhanced and sustained gene delivery, Pharm. Res. 24 (2007) 157–167.
[7] C.P. Lollo, M.G. Banaszczyk, H.C. Chiou, Obstacles and advances in non-viral gene delivery, Curr. Opin. Mol. Ther. 2 (2000) 136–142.
[8] A. Gautam, C.J. Waldrep, C.L. Densmore, Delivery systems for pulmonary gene therapy, Am. J. Respir. Med. 1 (2002) 35–46.
[9] O. Felt, P. Buri, R. Gurny, Chitosan: a unique polysaccharide for drug delivery, Drug Dev. Ind. Pharm. 24 (1998) 979–993.
[10] N. Csaba, A. Sanchez, E. Fernandez-Megia, R. Novoa-Carballal, M.J. Alonso, Chitosan nanoparticles for the delivery of plasmid DNA: preparation and characterization, Eur. J. Pharm. Sci. 23 (2004) 54.
[11] N. Csaba, M. Koping-Hoggard, E. Fernández-Mejía, R. Novoa-Carballal, R. Riguera, M.J. Alonso, Ionically crosslinked chitosan nanoparticles as gene delivery systems: effect of PEGylation on in vitro and in vivo gene transfer, J. Biomed. Nanotech., in press.
[12] H. Katas, H.O. Alpar, Development and characterisation of chitosan nanoparticles for siRNA delivery, J. Control. Release 115 (2006) 216–225.
[13] F. Maestrelli, M. García-Fuentes, P. Mura, M.J. Alonso, A new drug nanocarrier consisting of chitosan and hydroxypropylcyclodextrin, Eur. J. Pharm. Biopharm. 63 (2006) 79–86.

[14] A.H. Krauland, M.J. Alonso, Chitosan/cyclodextrin nanoparticles as macromolecular drug delivery system, Int. J. Pharm. 340 (2007) 134–142.
[15] A. Trapani, M. García-Fuentes, M.J. Alonso, Novel drug nanocarriers combining hydrophilic cyclodextrins and chitosan, Nanotechnology 19 (2008).
[16] S.-A. Cryan, A. Holohan, R. Donohue, R. Darcy, C.M. ÓDriscoll, Cell transfection with polycationic cyclodextrin vectors, Eur. J. Pharm. Sci. 21 (2004) 625–633.
[17] R. Challa, A. Ahuja, J. Ali, R.K. Khar, Cyclodextrins in drug delivery: an updated review, AAPS PharmSciTech 6 (2005) E329–E357 (http://www.aapspharmscitech.org).
[18] S.J. Hwang, N.C. Bellocq, M.E. Davis, Effects of structure of β-cyclodextrin-containing polymers on gene delivery, Bioconj. Chem. 12 (2001) 280–290.
[19] H. Arima, F. Kihara, F. Hirayama, K. Uekema, Enhancement of gene expression by polyamidoamine dendrimer conjugates with α-, β -, and γ-cyclodextrins, Bioconj. Chem. 12 (2001) 476–484.
[20] M.L. Forrest, N. Gabrielson, D.W. Pack, Cyclodextrin-polyethylenimine conjugates for targeted in vitro gene delivery, Biotechnol. Bioeng. 89 (2005) 416–423.
[21] B.I. Florea, C. Meaney, H.E. Junginger, G. Borchard, Transfection efficiency and toxicity of polyethylenimine in differentiated Calu-3 and nondifferentiated COS-1 cell cultures, AAPS Pharm. Sci. 4 (2002) E12 (http://www.aapspharmsci.org).
[22] A.M. De Campos, Y. Diebold, E.L.S. Carvalho, A. Sánchez, M.J. Alonso, Chitosan nanoparticles as new ocular drug delivery systems: in vitro stability, in vivo fate, and cellular toxicity, Pharm. Res. 21 (2004) 803–810.
[23] K.A. Janes, M.J. Alonso, Depolymerized chitosan nanoparticles for protein delivery: preparation and characterization, J. Appl. Polym. Sci. 88 (2003) 2769–2776.
[24] P. Calvo, C. Remuñán-López, J.L. Vila-Jato, M.J. Alonso, Novel hydrophilic chitosan-polyethylene oxide nanoparticles as protein carriers, J. Appl. Polym. Sci. 63 (1997) 125–132.
[25] M. De la Fuente, B. Seijo, M.J. Alonso, Design of novel polysaccharidic nanostructures for gene delivery, Nanotechnology 19 (2008).
[26] X.W. Li, D.K.L. Lee, A.S.C. Chan, H.O. Alpar, Sustained expression in mammalian cells with DNA complexes and chitosan nanoparticles, Biochim. Biophys. Acta 1630 (2003) 7–18.
[27] D. Teijeiro-Osorio, C. Remuñán-López, H.M. Nielsen, Comparative studies of chitosan nanoparticles and molecules in Calu-3 and TR146 cells, 32nd Ann. Meet. Exp. Control. Release Soc. 16 (2005) 378.
[28] G. Borchard, Calu-3 cells, a valid model for the airway epithelium?, ST.P. Pharm. Sci. 12 (2002) 205–211.
[29] C.I. Grainger, L.L. Greenwell, D.J. Lockley, G.P. Martin, B. Forbes, Culture of Calu-3 cells at the air interface provides a representative model of the airway epithelial barrier, Pharm. Res. 23 (2006) 1482–1490.
[30] M. Huang, Z. Ma, E. Khor, L.-Y. Lim, Uptake of FITC-chitosan nanoparticles by A549 cells, Pharm. Res. 19 (2002) 1488–1494.
[31] L. Paasonen, M. Korhonen, M. Yliperttula, A. Urtti, Epidermal cell culture model with tight stratum corneum as a tool for dermal gene delivery studies, Int. J. Pharm. 307 (2006) 188–193.
[32] M. De la Fuente, B. Seijo, M.J. Alonso, Bioadhesive hyaluronan–chitosan nanoparticles can transport genes across the ocular mucosa and transfect ocular tissue, Gene Ther. 15 (2008) 668–676.
[33] M. Koping-Hoggard, K.M. Varum, M. Issa, S. Danielsen, B.E. Christensen, B.T. Stokke, P. Artursson, Improved chitosan-mediated gene delivery based on easily dissociated chitosan polyplexes of highly defined chitosan oligomers, Gene Ther. 11 (2004) 1441–1452.